Geo-Marine Letters

Supporting Information for

Determining bubble size in aquatic sediments using wideband acoustic resonance and a bubble size distribution model: testing and application in Lake Kinneret, Israel

E. Uzhansky[1*], R. Katsman[1], A. Lunkov[2], B. Katsnelson[1]

[1] *Dr. Moses Strauss Department of Marine Geosciences, L. Charney School of Marine Sciences, University of Haifa, Haifa, Israel*

[2] *Prokhorov General Physics Institute of the Russian Academy of Sciences, Russia*

*Corresponding author email: ernstuzhansky@gmail.com

S1. Acoustic model input data, formulas and parameters

The following input data and expressions were utilized for calculations of sound speed in gassy, c_g, and gas-free, c_{gf}, aquatic sediments (Eq.7) and attenuation coefficient, α_g (Eq.8), in gassy sediments, with a histogram (discrete) distribution of gas bubbles sizes depicted in Figure 1c (following Anderson and Hampton 1980a, b; Gardner 2003; Best et al. 2004; Tõth et al. 2015 and references therein).

Table S1. Geoacoustic parameters and input data used for calculations.

Parameter	**Value**
Water depth	40[c,f] m
Depth of the gas horizon in the sediment below sediment-water interface	1 m
γ, Ratio of the specific heat capacity of methane gas at constant pressure to that at constant volume	1.333[a]
ρ_g, Density of gas (CH_4)	0.717[d] $\frac{kg}{m^3}$
ρ_r, Density of rigid particles in sediment	2200[c] $\frac{kg}{m^3}$
ρ_w, Density of water	1000[c] $\frac{kg}{m^3}$
C_g, Thermal conductivity of gas (CH_4)	0.0311[d,e] $\frac{J}{s\,m\,°C}$
E, Young's modulus (G, shear modulus) of water-saturated gas-free sediment	*209*[b] kPa (69.7 kPa)
G' imaginary part of complex shear modulus of water-saturated gas-free sediment, Pa.	25% of G[a]
n_r, Volume fraction of rigid particles in gas-free saturated sediment	0.4
n_w, Volume fraction of water in gas-free saturated sediment	0.6
K_r, Bulk modulus of rigid particles	19.6[c] GPa
K_w, Bulk modulus of water	2.25[c] GPa
s_p, Specific heat of gas (CH_4) at constant pressure	2.19[e] $\frac{kJ}{kg°C}$

[a]Anderson and Hampton (1980b), Gardner (2003)
[b]Barry et al. (2012), Katsman (2024)
[c]Katsnelson et al. (2017)
[d]Best et al. (2004)
[e]Tõth et al. (2015)

Table S2. Description of parameters used in the equations

Parameter	Description	Equation
α_g	sound attenuation coefficient in gassy sediment, *dB/m*	8
γ	ratio of the specific heat capacity of methane gas at constant pressure to that at constant volume	7, S5, S6
ρ	effective bulk density of gas-free sediment, $\frac{kg}{m^3}$	S1, S4
ρ_g	density of gas (methane), $\frac{kg}{m^3}$	S7
ρ_r	density of rigid particles in sediment, $\frac{kg}{m^3}$	S1
ρ_w	density of water, $\frac{kg}{m^3}$	S1
A	gas polytropic coefficient	S5
c_g	acoustic phase velocity in gassy sediment, *m/s*	7, 8
c_{gf}	acoustic phase velocity in gas-free sediment, *m/s*	7, 8, S1, S9
C_g	thermal conductivity of gas (methane), $\frac{J}{s\,m\,°C}$	S7
d	bubble damping constant	S8, S9
d_f	bubble damping due to fluid viscosity	S8, S9
d_r	bubble damping due to radiation	S8, S9
d_t	bubble damping due to thermal properties of gas	S8, S9
f	frequency of acoustic signal, *Hz*	8, S3, S4, S7, S9
f_0	resonance frequency, *Hz*	S4, S9
G	shear modulus of water-saturated gas-free sediment (the real part of the complex sediment shear modulus), *Pa*	7, 8, S4, S9
G'	imaginary part of complex shear modulus of water-saturated gas-free sediment, *Pa*.	S9
i	index of bubble size	S2-S9
K	Effective bulk modulus of water-saturated gas-free sediment, *Pa*	S1
K_r	Bulk modulus of rigid particles, *Pa*	S1
K_w	Bulk modulus of water, *Pa*	S1
M	Number of discrete bubble sizes	S2
n_g	volume fraction of gas	S3
n_r	volume fraction of rigid particles	S1
n_w	volume fraction of water	S1
P_0	ambient hydrostatic pressure, *Pa*	7, 8, S4
r	bubble equivalent spherical radius, *m*	S4, S7, S9
s_p	specific heat of gas (methane) at constant pressure, $\frac{J}{kg°C}$	S7
X_*, Y_*	frequency-dependent variables incorporating gas fraction and damping for a single gas bubble size	S2, S3
X_1, Y_1	frequency-dependent variables incorporating gas fraction and damping for a distribution of gas bubble sizes (Figure 1c)	7, 8, S2

Formulas for gas-free sediment

Acoustic phase velocity in gas-free sediment is evaluated as (Wood, 1955):

$$c_{gf} = \sqrt{\frac{K}{\rho}}, \tag{S1}$$

where $K = (n_r K_r^{-1} + n_w K_w^{-1})^{-1}$, $\rho = n_r \rho_r + n_w \rho_w$ are the bulk modulus and density, respectively, $n_r + n_w = 1$ is the total volume concentration of rigid particles and water.

Formulas used for calculations of sound speed, c_g, and attenuation, α, in gassy sediment (Eqs. 7,8) (description of used parameter values is presented in Table A2):

Variables X_1 and Y_1 are calculated as a sum over *M* discrete bubble sizes indexed by *i* (see Fig.2):

$$X_1 = \sum_{i=1}^{M} X_{*i} \quad , \qquad Y_1 = \sum_{i=1}^{M} Y_{*i} \tag{S2}$$

of the frequency-dependent variables, X_*, Y_*, specified for each single bubble size *i*:

$$X_{*i} = \frac{n_g(1 - f_{*i}^2)}{(1 - f_{*i}^2)^2 + d_{*i}^2}, \qquad Y_{*i} = \frac{n_g d_{*i}^2}{(1 - f_{*i}^2)^2 + d_{*i}^2} \tag{S3}$$

Resonance frequency, f_0, of a single bubble of size *i* in sediment, is calculated as:

$$f_{*i} = \frac{f}{f_{0i}}, \qquad f_{0i} = \frac{1}{2\pi r_i}\sqrt{\frac{3\gamma P_0}{A_i \rho} + \frac{4G}{\rho}}, \tag{S4}$$

where f is frequency of the acoustic signal.

Gas polytropic coefficient *A* is calculated as:

$$A_i = (1 + B_i^2)\left(1 + \frac{3(\gamma - 1)}{X_i}\frac{(\sinh(X_i) - \sin(X_i))}{(\cosh(X_i) - \cos(X_i))}\right), \tag{S5}$$

where

$$B_i = 3(\gamma - 1)\left(\frac{X_i(\sinh(X_i) + \sin(X_i)) - 2(\cosh(X_i) - \cos(X_i))}{X_i^2((\cosh(X_i) - \cos(X_i)) + 3(\gamma - 1)(\sinh(X_i) - \sin(X_i))}\right), \tag{S6}$$

and

$$X_i = r_i\sqrt{\frac{4\pi f \rho_g s_p}{C_g}}, \tag{S7}$$

Damping, d_{*i}, of a single bubble size (indexed by *i*) is composed of damping due to thermal properties of gas d_{ti}, damping due to radiation d_{ri} and damping due to fluid viscosity d_{fi}:

$$d_{*i} = d_i f_{*i}^2, \qquad d_i = d_{fi} + d_{ti} + d_{ri}, \tag{S8}$$

$$d_{fi} = \frac{G'}{\pi^2 \rho f_{0i}^2 r_i^2}, \qquad d_{ti} = B_i, \qquad d_{ri} = \frac{2\pi f r_i}{c_{gf}}. \tag{S9}$$

Parameters used for the calculations are presented in Table S2. Constants are borrowed from studies that used a histogram-based bubbles sizes distribution model (following Anderson and Hampton 1980a, b). Elastic constants are borrowed from the similar shallow environments.

S2. Parameters of the sound speaker used and experimental results

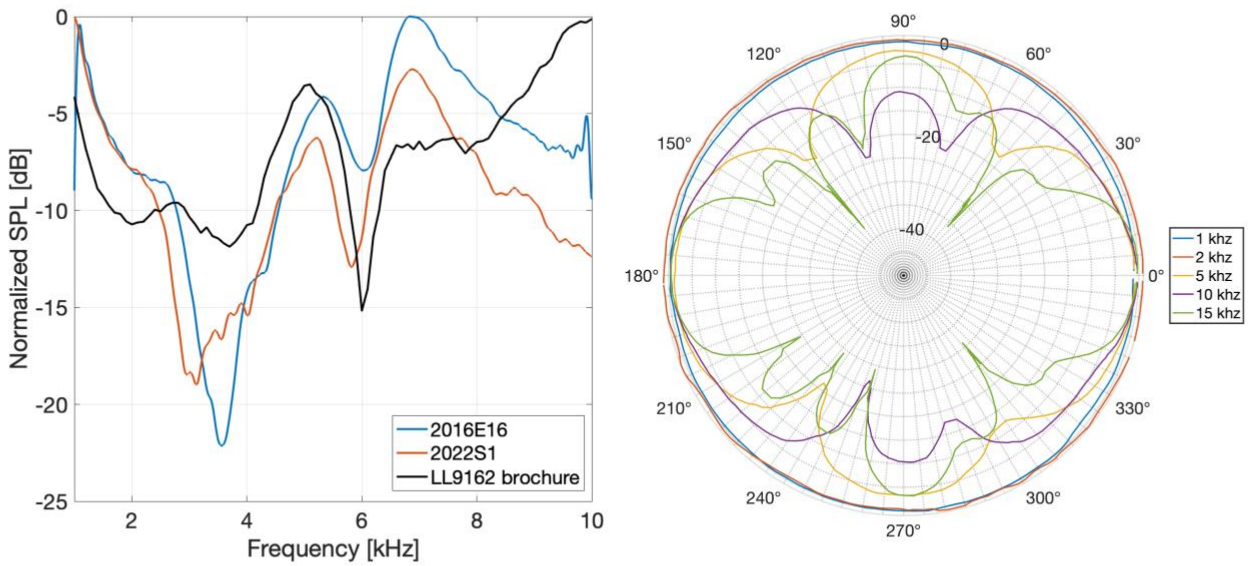

Figure S1. Parameters of the sound speaker LUBELL LL-9162T. (Right) Frequency response of the speaker, experimentally measured in 2016 (blue) and 2022 (red) experiments, and provided by the manufacturer (black). (Left) directivity decay pattern the speaker provided by the manufacturer.

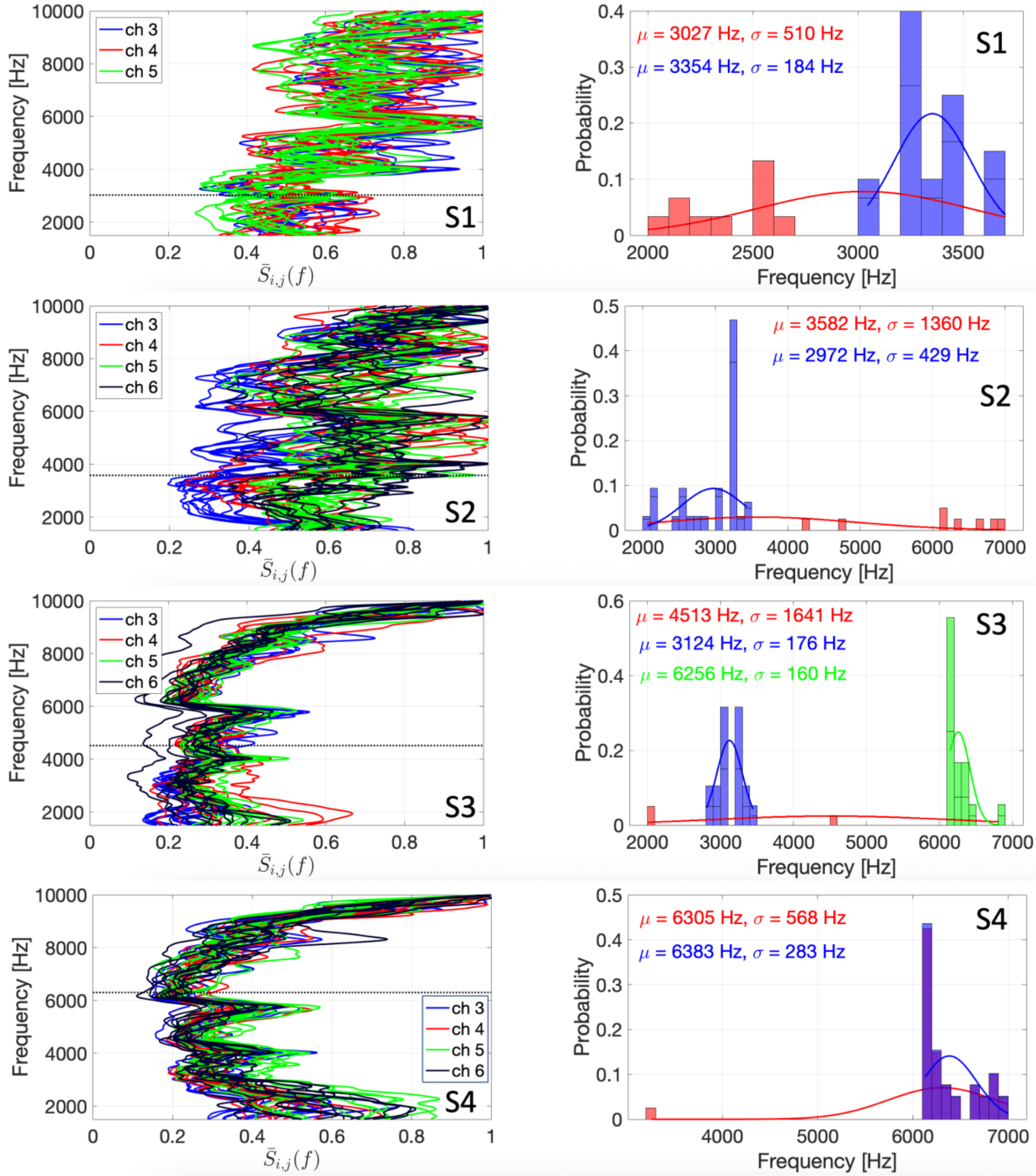

Figure S2. Results of the acoustic data analysis from the 2022 experiment from points S1 – S4. Left: time-averaged spectra of the reflected signals. Different channels are color coded. Dotted line depicts the mean f_{min} value from all samples. Right: histograms of f_{min} normal distribution fit showing its mean value, μ, and standard deviation, σ. Histogram and fit calculated for all samples are shown in red, with other colors being related to smaller individual groups (colors are matching between the color of the histogram, fit and text with μ and σ).

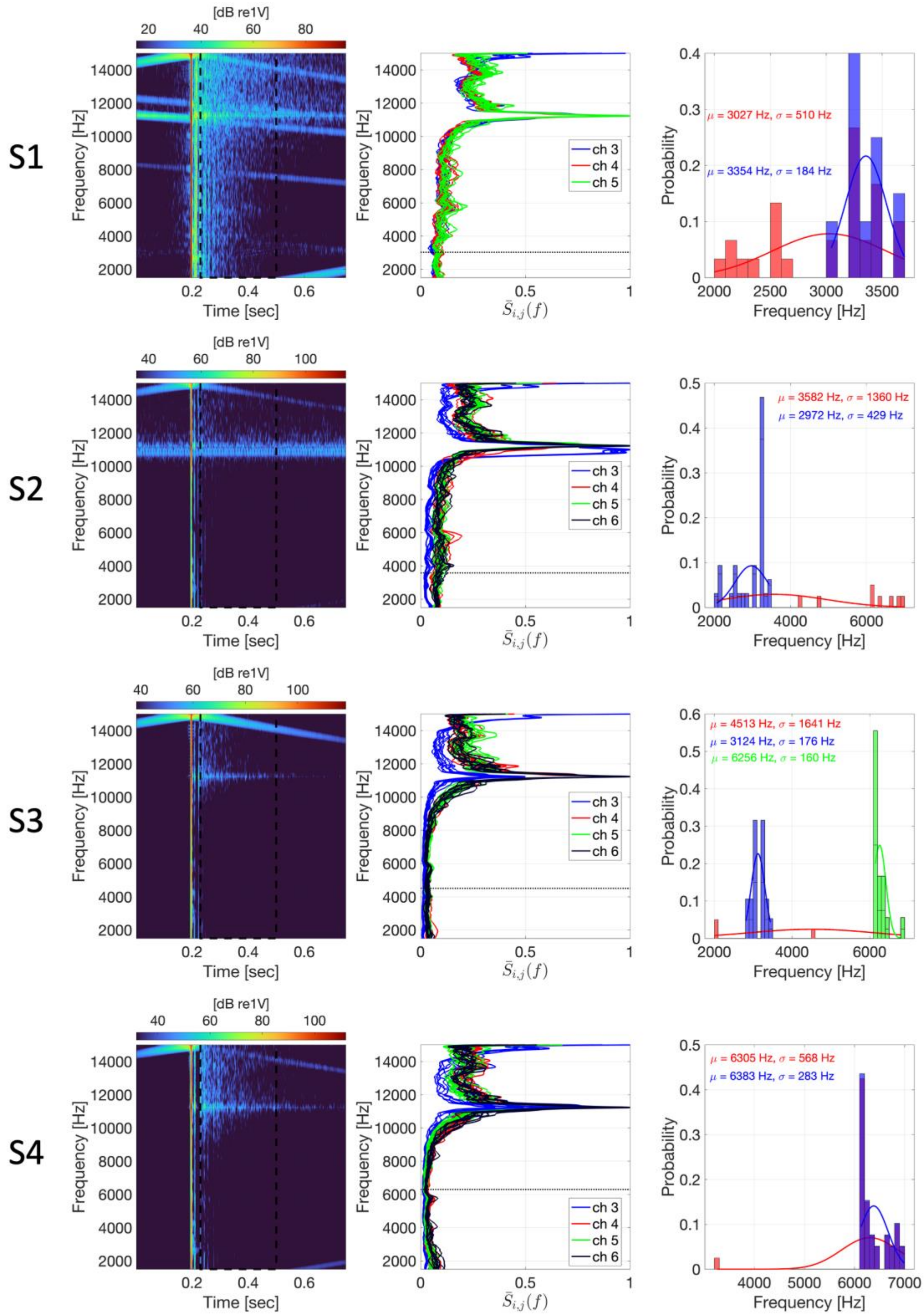

Figure S3. Results of the acoustic data analysis from the 2022 experiment from points S1 – S4 in the frequency band of up to 15000 Hz. Subplots obtained in the same manner as described in Figure 4 in the manuscript.